# Polar Low genesis over North Pacific under different scenarios of Global Warming

Fei Chen[1,2], Hans von Storch[1], Yan Du[3], Lun Wu[1]

1. Institution of Remote Sensing and Geographical Information System, School of Earth and Space Sciences, Peking University, Beijing, China

2. Helmholtz-Zentrum Geesthacht, Max-Planck-Str. 1, Geesthacht, Germany

3. South China Sea Institute of Oceanology, Chinese Academy of Science, Guangzhou, China

## Abstract:

Following an earlier climatology study of North Pacific Polar Lows by employing a dynamical downscaling of NCEP 1 reanalysis using the regional climate model COSMO-CLM, the characteristics of Polar Low genesis under different global warming scenarios are investigated. Three SRES scenarios run with a global climate model (ECHAM5) are examined if we may expect systematic changes in the formation of Polar Lows over the next century. The results show that with more greenhouse gas emission, global warming and the air temperature rising, the frequency of Polar Lows is decreasing. With sea ice melting, the distribution of Polar Low genesis shows a northward shift. In scenarios with stronger warming, the trend towards less Polar Lows gets larger.

## 1.Introduction

The North Pacific is an area where frequently sub-synoptic Polar Lows form in the cold season (Rasmussen and Turner 2003) in association with cold air outbreak. Because of the strong wind speeds and heavy rainfall, Polar Lows represent a significant weather climate risk which threats maritime human activities.

Multi-decadal reanalysis, such as those provided by NCEP or ECMWF, as well as climate change scenarios, as those in the CMIP ensembles, do not allow the determination of changing statistics of Polar Lows, because the spatial sale of these disturbances is insufficiently resolved in such data sets. Therefore dynamical downscaling efforts have been carried out, which employ regional climate models, to determine the multi-decadal climatology of Polar Lows (Chen and von Storch 2013). To do so, a regional climate model was conditioned by large-scale information of NCEP re-analyses. It turned out that in this way the formation and life cycles of Polar Lows during the past decades could be reconstructed homogeneously without exploiting sub-synoptic information in initial fields (Chen et al. 2012).

This approach is now used to determine, how the frequency of emergence of Polar Lows is changing in a series of scenarios describing the response of the climate system to three SRES

emission scenarios from the Intergovernmental Panel on Climate Change (IPCC) developed for the Assessment Reports 3 and 4.

In section 2 we briefly describe the data and methodology of the simulation and tracking algorithm. Section 3 is divided into three parts in order to determine (decreasing) trends in discuss the Polar Low genesis, variations of the trend associated with different greenhouse gas emission scenarios and the spatial (northward) shift of Polar Low genesis. The paper is concluded with a discussion and summary in the final section 4.

# 2. Methodology and data

**Downscaling and tracking**

The basic concept is to dynamically downscale scenario simulations with a global model for the region of the North Pacific. For doing so, the COSMO-CLM (Steppeler et al. 2003) was used as regional climate model. The COSMO-CLM (COSMO model in CLimate Mode) is the climate version of the operational weather prediction model of the Deutscher Wetterdienst and the COnsortium for SMall scale MOdelling (COSMO), adapted to climate simulation purposes by the CLM-Community (http://www.clm-community.eu).

The states in the global climate change simulations are fed into the regional model at the lateral boundaries and lower boundary. Similar as a previous climatological study (Chen and von Storch, 2013), which downscaled NCEP 1 reanalyses, the spectral nudging is employed also.

The CCLM model is capable to generate Polar Lows, without providing seeds in initial states (Chen et al., 2012). These Polar Lows are detected and tracked by using a modified algorithm developed by Zahn and von Storch (2008). For detailed information of the model, the downscaling technology and the tracking algorithm the reader is referred to the previous study (Chen et al. 2012; Chen and von Storch 2013).

**Scenario Information**

The scenarios we applied here are designed by the IPCC in 2000 (Nakicenovic et al. 2000) known as the Special Report on Emissions Scenarios (SRES). The SRES scenarios consider a wide range of factors, such as population, industrialization, urbanization, social and economic developments to estimate the greenhouse gas emission. These emission scenarios are fed into global climate models for studying the effect of increasing greenhouses gas concentrations on the possible future state of the climate system,, such as: investigating the changes of storm and cyclone activity under different SRES scenarios (Pinto et al. 2007) and increased precipitation intensity (Meehl, Arblaster, and Tebaldi 2005). Various characteristics which reflected the response of the climate system to different scenarios are also investigated and described by the scientists. Such as: the air temperature, precipitation, sea level raise, sea ice melting, ocean current circulation change, extremely weather phenomenon, aerosols and carbon dioxide cycle variability in climate (Stocker and Schmittner 1997; Boer, Flato, and Ramsden 2000; Cox et al. 2000; Friedlingstein et al. 2001; Yonetani and Gordon 2001).

**Forcing data: ECHAM5**

The global climate model used was the coupled GCM ECHAM5/MPI-OM1 (Roeckner et al. 2003) which refers the European Centre Hamburg Version 5/Max-Planck-Institute – Ocean Model Version 1. Detailed information is available in the documentations (Roeckner et al. 2003; Marsland et al. 2003; Jungclaus et al. 2005). The different scenario runs were initiated in the year "1948" and run until "2000" with observed forcing, and then the scenario-runs were extended until 2100. Three such simulations with A1B, labeled A1B_1, A1B_2 and A1B_3, were run with ECHAM5/MPI-OM and then dynamically downscaled with CCLM. Similarly one scenario exposed to B1 and A2 emission scenarios were processed. The output of the global runs was archived by CMIP5.

# 3. Simulation and tracking results

Polar Lows form in winter, therefore the "Polar Low season" (PLS) is defined as extending from October through next April. The Polar Low season is addressed by the first and second year, for example the PLS 2001/2002 begins in October 2001 and ends in April 2002. For each PLS we present in the following the number of detected North Pacific Polar Lows.

## 3.1 Analysis of A1B scenarios

For demonstrating the effect of the increasing $CO_2$ concentrations to the frequency of North Pacific Polar Lows formation, we take A1B as example. Figure 1a presents the time series of detected Polar Lows per PLS and the corresponding trend over the next century under the three realizations of A1B. They all share a negative trend and there is no obvious significant difference between the three realizations. Namely the trend for A1B_1 is -0.29 cases/PLS; for A1B_2 is -0.24 cases/PLS and for A1B_3 is -0.25 cases/PLS, with a corresponding standard deviation of 18.19, 16.12 and 17.49.

Figure 1b shows running 50 years trends of the three 2000-2099 series with A1B scenarios. The downturn of the number of cases varies somewhat in time, but is steady. When examining 30 and 40 years trends (not shown), a similar situation emerges, even though the variability of the series becomes much larger.

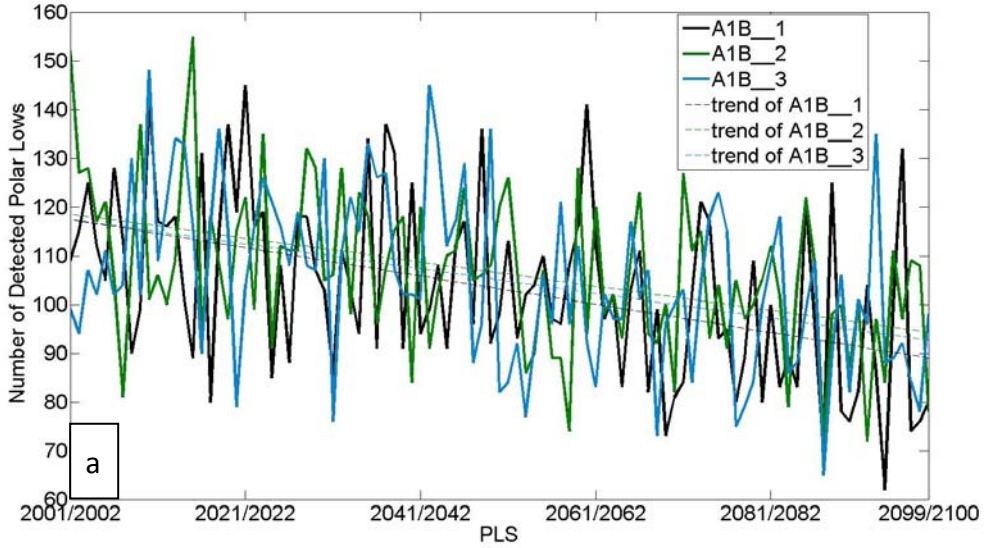


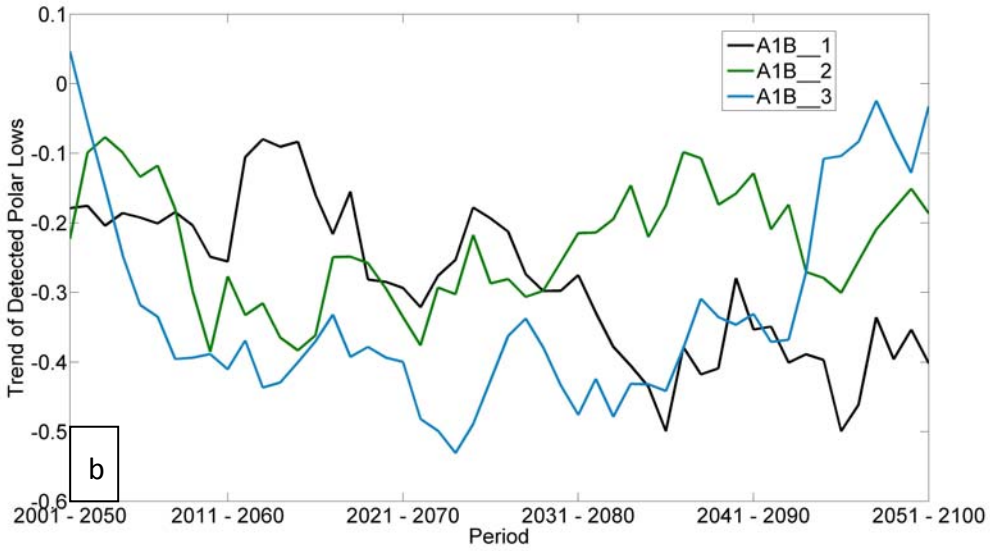


*Figure 1 a) Number of Detected Polar Lows per PLS simulation) and three realizations of A1B scenario, 2001/2002 – 2009/2100. The straight lines represent the trends for the three A1B developments. b) Running 50-years trends of the three combined series of detected Polar Lows per PLs in A1B; the trends are labeled with the first year of the mowing 50 year window.*

As Zahn and von Storch (2010) pointed out for the Polar Low frequency over the North Atlantic in the next century, that both the SST of the Atlantic and the tropospheric air temperature are getting warmer. However, the rise of tropospheric air temperature is higher than the rise of the SST, so that the troposphere-sea temperature difference is getting smaller, so that the vertical stability is getting higher. The increased stability is less favorable for Polar Low genesis. To demonstrate that this mechanism is also operating in the North Pacific, we determined the

seasonal temperature difference between the 500 hPa level and the seas surface for A1B_1. Only points with open water, i.e., no sea ice, were considered. We count the number of points for each PLS, where the mean air-sea temperature is equal or larger than 39 K. When this is the case we refer to “critical temperature difference”

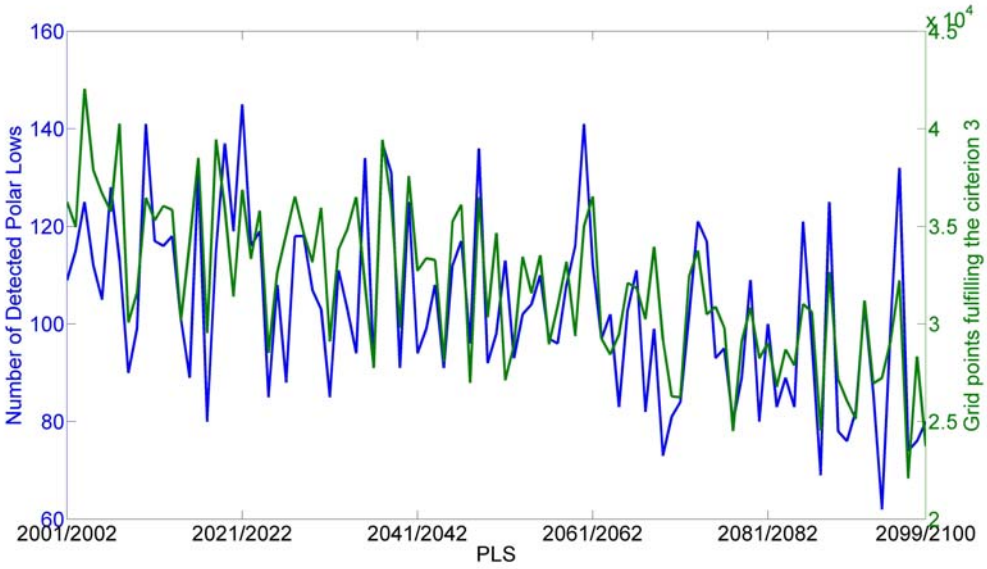


*Figure 2: Development of PLS-number of Polar Lows, derived from detecting and tracking (in blue) and percentage of open-sea grid points, with a vertical temperature gradient beyond the critical 39K (red).*

Since the number of points without sea ice is increasing, we show in Figure 2 the percentage of such points with a critical vertical temperature difference compared to the overall number of eligible (ice free sea) points. For A1B_1 this percentage decreases by 29% to the end of 21$^{th}$ century compared to the beginning (the corresponding trend is -93.53 grid points per PLS), for A1B_2 and A1B3 it is 24% with -71.31 grid points/PLS and 22% with -70.14 grid points/PLS. Thus, favorable conditions for Polar Low genesis decreased nearly one third since the beginning of this century for all three realizations of A1B simulations. The comparison with the directly detected and tracked Polar Lows, also shown in Figure 2, confirms that the proxy “Vertical temperature difference” describes adequately the decreasing trend in Polar Low activity for the 21$^{th}$ century: The correlation between the two curves, after subtraction of their trends, amounts to 74.4%. For A1B_2 it is 72.8%, for A1B_3 is 79.1% (not shown)

# 2 Other Greenhouse Gas emission scenarios

As shown in Figure 1a, there is no obvious significant difference between different realizations of single story line. Therefore and for reasons of computational cost and time we only take the first realization for the different scenarios such as A2_1 and B1_1. In the following we refer only to A1B, A2 and B1.

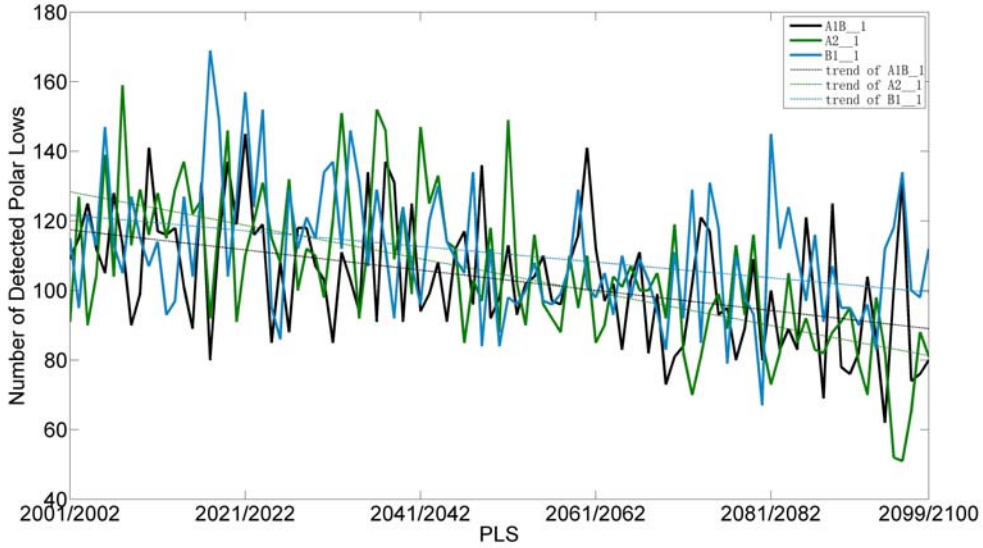


*Figure 3: Number of Detected Polar Lows and corresponding trends from 2001/2002 to 2099/2100 of A1B, A2 and B1.*

Figure 3 presents the different tracking results for the three different emission scenarios. In all, the number of Polar Lows is decreasing: The trend of A1B is -0.29 case/PLS; for the scenario of A2, which has a much higher greenhouse gas emission, the trend is -0.49 cases/PLS. For B1_1 the trend is much smaller, with only -0.2 case/PLS. We find that with a higher greenhouse gas emission, the frequency of Polar Low occurrence has a correspondingly stronger decreasing trend. This is also supported by a general decrease of grid points where the mean vertical temperature is beyond the critical 39K (not shown).

We have inferred that there will be a lower trend of Polar Low occurrence frequency over the North Pacific in the next century under a global warming situation with a higher greenhouse gas emission. The higher air temperature raise, the lower air-sea temperature differences drop. Consistently, the frequency of favorable conditions for Polar Low genesis is declines (Figure ).

## 3.3 Northward shift of Polar Low genesis associated with ice edge melting

For the next step, we are interested on the spatial distribution of Polar Low genesis and its variability under future global warming scenario. Here we take A1B as an example. For doing so, the North Pacific was divided into 12 sub-regions to compare the Polar Low information in different areas. The same sub-regions have been used by Chen and von Storch (2013) to describe the present spatial statistics of the formation of Polar Lows. The density of Polar Low genesis, the trends in number and in changes of the vertical stability, as well as the correlation of the two

measures of Polar Low genesis in the 12 sub-regions in the next century are presented in Figure 4.

The region of highest Polar Low density is located to the east ocean of Japan Island (R9), the smallest values in R21 in the far southwest, and R6 and R7 in the southeast - in consistence with the climatology of last six decades. The most trends are in all 12 sub-regions negative, both in terms of detected and tracked polar lows, and in terms of the proxy "spatial percentage of critical vertical temperature difference" (in R2 the trend is small, albeit positive). The two measures are all positively correlated (after taking out the trends), with a maximum of 60% in R4 west of the dateline and a minimum 8% in R12 in the far southwest of the area.

The strongest decline trend of Polar Lows genesis per open-sea grid point is found in R9 east of Japan with $-6.9 \times 10^{-2}$ cases per grid point per PLS. In R4 the trend is with $-4.8 \times 10^{-2}$ cases per grid point per PLS. For the sub-regions R1, R5, R6 and R11, the trends in detected and tracked Polar lows is about $2 \times 10^{-2}$ cases per open-sea grid point per PLS; in the other sub-regions the trends are smaller.

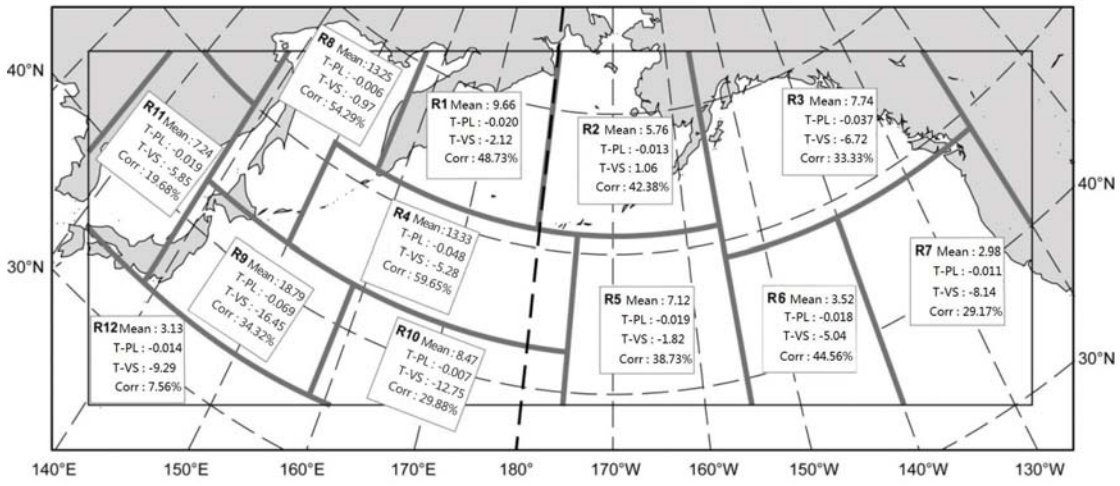


*Figure 4: Sub-regions, for which the numbers (Mean) of and trends in detected (T-PL), or estimated (T-VS) Polar Lows formation were aggregated (R1-R12). Also given are the correlations (corr) between the detected and estimated Polar occurrence (after subtracting trends). The estimated number is the percentage of open-sea grid points in each sub-region, where the critical temperature difference between the sea surface and 500 hPa of 39K or more is met.*

The correlated measure of percentage of open-sea points with a vertical difference of 39K and beyond shows a similar pattern, with mostly negative trends (labeled T-VS in Figure 4), but one, albeit very small positive trend in R2. In general, the trends in the Northwest, in R1, R2 and R8, exhibit small trends, while in the other sub-regions the trends are solidly negative, with largest values in R9 and R10.

The correlation of the 12 trends, derived from the tracking data, and derived from the change in vertical temperature differences, amounts to 43%.

Another similar measure is the trend in the number of times, on the basis of four-times daily grid point data, per PLS with a critical temperature difference of 39 K and more (Figure 5). (Before, we had examined the percentage of points with a critical difference in the seasonal mean; here we determine the change of the percentage in time per PLS.) The frequency of relatively more stable conditions, when the 39 K difference is not met, increases almost everywhere in the North Pacific Basin, with maximum values of -0.5 grid points/PLS east of Japan – but also larger regions in the North. Consistently the largest differences in the emergence of Polar Lows are in the Northwest Pacific, and the weakest are where red colors dominate in Figure 5. The tendency towards more stable conditions in most of the region reflects the faster warming of the troposphere, and the slower warming at the sea surface. The red regions point to the retreat of sea ice in the course of the overall warming (Figure 6).

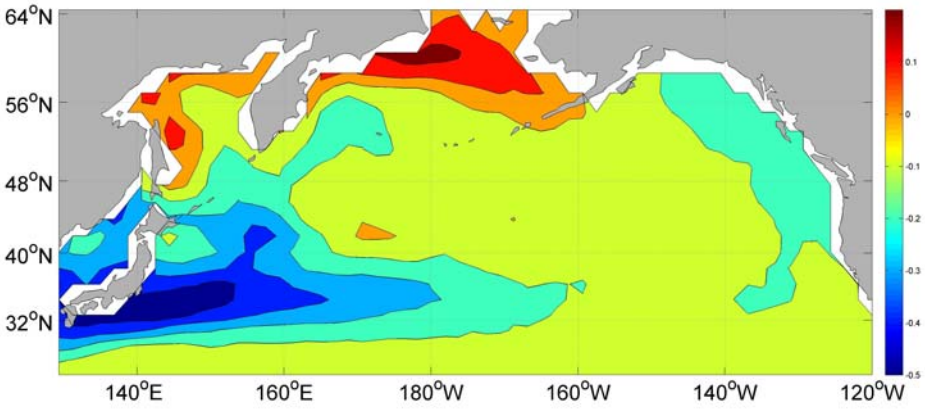


*Figure 5: Trends of the frequency of number of times (of 4-times daily values) within a PLS, when the vertical temperature difference (SST – 500 hPa temperature) is 39K or more. Red colors point to more frequent more stable conditions, while blue indicate less frequent such conditions. Units: grid points/PLS.*

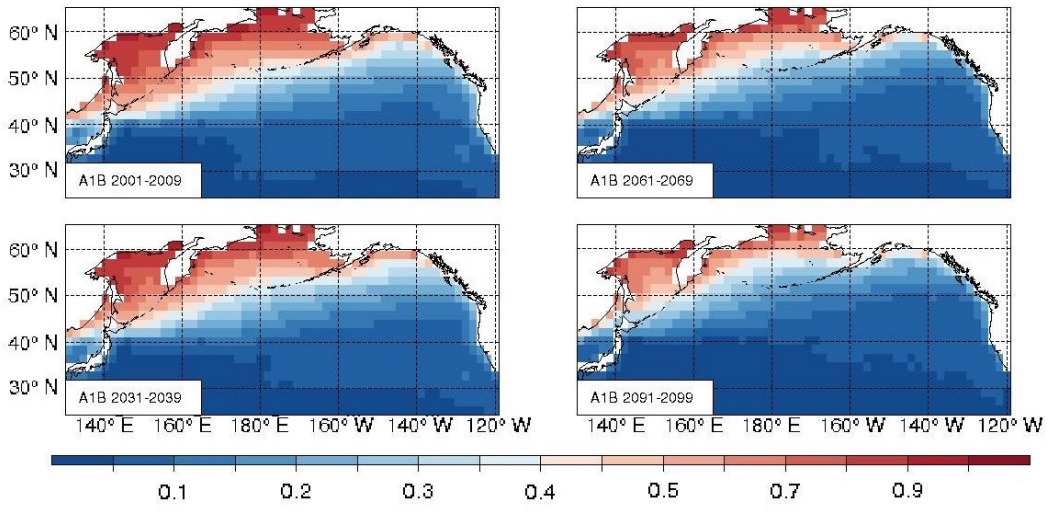


*Figure 6: Mean proportion of ice covered time over the North Pacific Ocean during the PLS for different 10 year means: 2001-2009, 2031-2039, 2061-2069 and 2091-2099 are calculated from the ECHAM5/MPI-OM1 of A1B_1.*

Figure 6 demonstrates this gradual decrease of the sea ice in the northern parts of the region. During the first decade, 2001-1009, sea ice is present in most part of the sea of Okhotsk and Bering Sea during 70% of a PLS. In the Gulf of Alaska also nearly 50% of the time the sea is frozen along the north coast. But for the last 70 PLSs during 2031 – 2099, the proportion of sea ice during winter is gradually decreasing. In the Okhotsk and Bering Sea and in the Gulf of Alaska, the time of frozen conditions is dropped by 55% at the end of next century in this scenario.

When the sea ice edge is retreating, the cold air flow from the north meets the relative warm SST earlier on its southward movement. Thus, in these regions, such as R1 and R8, the reduction of numbers of Polar Lows is smallest. At the same time, the cold continental air has to travel a longer distance across the warmer SST before reaching the more southern regions, so that there the tendency for forming Polar Lows in R4 and R9 is further reduced.

For comparing the strengths of the trends between the sub-regions, we calculated area weighted mean of their trends by divided the overall trends by the number sea grid points for each sub-region. The overall trend of detected Polar Lows is negative with -0.29 cases/PLS, which am amounts to $-2.7\times10^{-5}$ cases per PLS per grid point. The trends in different sub-regions are not uniform. R9 exhibits the strongest decrease trend of $-8.3\times10^{-5}$ cases per PLS per grid point. For R1, R4 and R11 somewhat smaller decreasing trends prevail: $-2.0\times10^{-5}$, $-4.8\times10^{-5}$, and $-6.9\times10^{-5}$. The R8-trend is the weakest $-0.9\times10^{-5}$ cases per PLS per grid point. This pattern describes a relative northward shift of Polar Low distribution in the coming 100n years of the scenario A1B.

In the A2 and B1 scenarios the changes of sea ice melting and a northward shift of Polar Low formation are similar to A1B (not shown). With more or less $CO_2$ emission and global warming, the Polar Low formation appears to migrate more, or less, northward.

# 4. Conclusion

We applied global climate model products under different scenarios of societal development in the future, which go along with different greenhouse gas emissions and global warming developments. Corresponding spatial distribution of genesis and the trend of Polar Low occurrence frequency are calculated by a model-based methodology which we had developed for a hind cast of the last 62 years conditions 1948 to 2010 (Chen and von Storch, 2013).

A general idea is that the frequency of Polar Low occurrence has a close relationship with the global warming. With a stronger increase of the $CO_2$ emission the frequency is decreasing much more rapidly than with smaller increases. The spatial distribution shows a northward shift through next century under the different scenarios. The explanation for this change is mainly related to the raised atmosphere temperatures, less fast warming of the srea surface and a gradual retreat of the northern ice cover. The decrease of air-sea temperature difference leads to reduced vertical instability. With less frequent favorable condition, the frequency of Polar Low occurrence is decreasing; with melting sea ice and northward ice edge, the Polar Lows forms more northward compared than in earlier times.

We have to point out that our regional simulation is a scenario, i.e., a possible and consistent description of future conditions related only to greenhouse gas and aerosol emissions, but not a prediction of what may be considered the most probable development expected to happen in the coming 90 years.

# Acknowledgement

The work was done with the support of the Chinese Scholarship Council CSC, and it is a contribution to the Helmholtz Climate Initiative REKLIM (Regional Climate Change), a joint research project of the Helmholtz Association of German Research Centers. The authors thank Beate Gardeike for preparing most of the diagrams. The technical and scientific support, the various comments and suggestions by Dr. Beate Geyer and Dr. Matthias Zahn have greatly improved this manuscript.

# Reference

Boer, G.J., G. Flato, and D. Ramsden, 2000: A Transient Climate Change Simulation with Greenhouse Gas and Aerosol Forcing: Projected Climate to the Twenty-first Century. Climate Dynamics 16: 427–450.

Chen, Fei, Beate Geyer, Matthias Zahn, and Hans von Storch, 2012: Towards a Multi-Decadal Climatology of North Pacific Polar Lows Employing Dynamical Downscaling. Terr. Atmos. Ocean. Sci. 23(3): 291–301.

Chen, Fei, and Hans von Storch, 2013: Trends and Variability of North Pacific Polar Lows. Advances in Meterology. http://dx.doi.org/10.1155/2013/170387

Cox, P.M., R.A. Betts, C.D. Jones, S.A. Spall, and I.J. Totterdell, 2000: Acceleration of Global Warming Due to Carbon-cycle Feedbacks in a 3D Coupled Climate Model. Nature 408: 184–187.

Friedlingstein, P., L. Bopp, P. Ciais, et al., 2001: Positive Feedback Between Future Climate Change and the Carbon Cycle. Geophys. Res. Lett 28(8): 1543.

Jungclaus, J.H., M. Botzet, H. Haak, et al., 2005: Ocean Circulation and Tropical Variability in the Coupled Model. ECHAM5/MPI-OM. J. Climate 19: 3952–3972.

Marsland, S.J., H. Haak, J.H. Jungclaus, M. Latif, and F. Röske, 2003: The Max-Planck-Institute Global Ocean/sea Ice Model with Orthogonal Curvilinear Coordinates. Ocean Model 5: 91–127.

Meehl, Gerald A., Julie M. Arblaster, and Claudia Tebaldi, 2005: Understanding Future Patterns of Increased Precipitation Intensity in Climate Model Simulations. Geophys. Res. Lett. 32: L18719.

Nakicenovic, N., J. Alcamo, G. Davis, et al., 2000: Special Report on Emissions Scenarios: a Special Report of Working Group III of the Intergovernmental Panel on Climate Change. http://www.ipcc.ch/ipccreports/sres/emission/index.php?idp=0.

Pinto, J. G., U. Ulbrich, G. C. Leckebusch, et al., 2007: Changes in Storm Track and Cyclone Activity in Three SRES Ensemble Experiments with the ECHAM5/MPI-OM1 GCM. Clim. Dynam. 29: 195–210.

Rasmussen, Erik A., and John Turner, 2003: Polar Lows: Mesoscale Weather Systems in the Polar Regions. Cambridge University Press.

Rockel, Burkhardt, Christopher L. Castro, Roger A. Pielke Sr., Hans von Storch, and Giovanni Leoncini, 2008: Dynamical Downscaling: Assessment of Model System Dependent Retained and Added Variability for Two Different Regional Climate Models. Journal of Geophys. Res. 113.

Roeckner, E., G. Bauml, L. Bonaventura, et al., 2003: The Atmospheric General Circulation Model ECHAM5. PART I: Model Description. Hamburg: Max-Planck-Institut für Meteorologie.

Roeckner, Erich, Michael Lautenschlager, and Heiko Schneider, 2006:IPCC-AR4 MPI-ECHAM5_T63L31 MPI-OM_GR1.5L40 SRESA1B Run No.1: Atmosphere 6 HOUR Values MPImet/MaD Germany. World Data Center for Climate. http://dx.doi.org/10.1594/WDCC/EH5-T63L31_OM-GR1.5L40_A1B_1_6H.

2006a IPCC-AR4 MPI-ECHAM5_T63L31 MPI-OM_GR1.5L40 SRESA1B Run No.2: Atmosphere 6 HOUR Values MPImet/MaD Germany. World Data Center for Climate. http://dx.doi.org/10.1594/WDCC/EH5-T63L31_OM-GR1.5L40_A1B_2_6H.

2006b IPCC-AR4 MPI-ECHAM5_T63L31 MPI-OM_GR1.5L40 SRESA1B Run No.3: Atmosphere 6 HOUR Values MPImet/MaD Germany. World Data Center for Climate. http://dx.doi.org/10.1594/WDCC/EH5-T63L31_OM-GR1.5L40_A1B_3_6H.

2006d IPCC-AR4 MPI-ECHAM5_T63L31 MPI-OM_GR1.5L40 SRESA2 Run No.1: Atmosphere 6 HOUR Values MPImet/MaD Germany. World Data Center for Climate.

http://dx.doi.org/10.1594/WDCC/EH5-T63L31_OM-GR1.5L40_A2_1_6H.

2006e IPCC-AR4 MPI-ECHAM5_T63L31 MPI-OM_GR1.5L40 SRESB1 Run No.1: Atmosphere 6 HOUR Values MPImet/MaD Germany. World Data Center for Climate. http://dx.doi.org/10.1594/WDCC/EH5-T63L31_OM-GR1.5L40_B1_1_6H.

Steppeler, J, G Doms, U Schättler, et al., 2003: Meso-gamma Scale Forecasts Using the Nonhydrostatic Model LM. Meteorology and Atmospheric Physics 82(1): 75–96.

Stocker, T. F., and A. Schmittner, 1997: Influence of CO2 Emission Rates on the Stability of the Thermohaline Circulation. Nature 388: 862–865.

Yonetani, T., and H.B. Gordon, 2001: Simulated Changes in the Frequency of Extremes and Regional Features of Seasonal/Annual Temperature and Precipitation When Atmospheric CO2 Is Doubled. Journal Of Climate 14(8): 1765–1779.

Zahn, M., and H. von Storch, 2008: Tracking Polar Lows in CLM. Meteorologische Zeitschrift 17(4): 445–453.

Zahn, Matthias, and Hans von Storch, 2010: Decreased Frequency of North Atlantic Polar Lows Associated with Future Climate Warming. Nature 467(7313): 309–312.